4027

Predicting DTI Tractography Uncertainty from Diffusion-Weighted-Image Noise

Jadrian Miles[1], and David H. Laidlaw[1]

[1]*Computer Science Department, Brown University, Providence, Rhode Island, United States*

Introduction — This work presents a simple method to compute the uncertainty of diffusion-tensor tractography streamlines from the noise properties of the source DWIs, and finds that the radius of uncertainty about a streamline increases with the square root of arc-length distance from the seed point. We empirically derive the statistical uncertainty model from Monte-Carlo studies of tensor reconstruction and tractography under noise.

Methods — We generated 13 randomly-oriented smooth fields of synthetic axially-symmetric diffusion tensors, and generated synthetic noise-free diffusion-weighted images from the tensors. Parameter values were FA = 0.85, MD = 0.00070 mm^2/s, and I_0 = 290; the voxels were nominally 2mm per side in a 25x25x25 grid. We generated the noise-free DWIs for five independent sets of uniformly-distributed b-vectors at b = 1000 s/mm^2, with n_b = {6,16,32,64,128} vectors. We added synthetic Rician noise in five repetitions at five different noise levels, σ_n = {4,10,18,28,40}, corresponding to SNRs of 13.9–1.4 axially and 58.0–5.8 orthogonally.

Experiment 1 — For each set of noisy DWIs, we fit diffusion tensors by linear least-squares solving of the log of the Stejskal-Tanner equation. We computed the angles between the principal eigenvectors of the noise-free and reconstructed tensors.

Experiment 2 — For each set of DTIs, we performed tractography via adaptive fifth-order Runge-Kutta integration [1] with cubic interpolation over the field of principal eigenvectors, with a fixed set of 500 uniform random seed points. Thus each seed point in each vector field generated one noise-free streamline and 125 noisy streamlines. We parameterized positions on each curve by signed arc-length distance from the seed. Autocorrelation analysis indicated that the angle between the tangents at corresponding positions on noise-free and noisy streamlines was independent when sampled every 4mm (twice the voxel width).

For each corresponding pair of noise-free and noisy 4mm streamline segments, we measured three values: (1) the initial orthogonal offset, $off_{\perp,i}$: the distance between the initial endpoints of the segments as projected into the plane orthogonal to the initial tangent vector of the noise-free segment; (2) the similarly-defined final orthogonal offset, $off_{\perp,f}$; and (3) the initial orthogonal divergence, $div_{\perp,i}$: the divergence of the projection of the noise-free principal eigenvector field into the plane orthogonal to the initial noise-free tangent vector.

Results — Histograms of angular differences in Experiment 1 exhibit a Rayleigh distribution (Figure A). Plotting n_b, σ_n, and the Rayleigh-fit scale parameter σ_θ in log-space (Figure B), we find $\sigma_\theta = 0.0124\ \sigma_n / \sqrt{(n_b)}$. Histograms of $off_{\perp,f}$ from Experiment 2 are well-described by Rician distributions with offset $\nu = |off_{\perp,i}|$ and scale $\sigma = 0.0164\ \sigma_n / \sqrt{(n_b)}$ (Figure C), with no dependence on $div_{\perp,i}$.

Discussion — The results described above match the theoretical expectation for small-magnitude random normal orthogonal deviations of a vector, in which the unit sphere near the tip of a unit vector is approximated by a plane. This approximation was valid even at σ_n = 40. The uncertainty in the advection process, then, may be thought of as a set of probability distributions in planes orthogonal to the streamline. At the seed, it is a Dirac delta distribution, and successive 4mm steps iteratively convolve each distribution with a Gaussian. At 4*n* mm along the curve from the seed, then, the uncertainty distribution in the orthogonal plane is a circular bivariate Gaussian with standard deviation $0.0164 \sqrt{(n)}\ \sigma_n / \sqrt{(n_b)}$, where σ_n may be estimated from a sample of *N* DWI background voxel intensities I_j as $\sigma_n \approx \sqrt{(\sum I_j^2 / 2N)}$.

We observed heavier tails in Experiment 1 for the n_b = 6 cases than a Rayleigh distribution. This is likely due to the "attractive orientation" effect described by Laun, et al. [2]. For higher n_b, this effect disappears and the Rayleigh model fits well.

For the range of values we observed in significant quantities in Experiment 2, the maximum $off_{\perp,i}$ was 1mm and the maximum $div_{\perp,i}$ was 0.08. The results indicated no dependence on $div_{\perp,i}$, but we would expect an effect for higher values of $off_{\perp,i}$ (around 4mm) and $div_{\perp,i}$ (as in fanning or branching regions). Large-scale deviation due to tissue variation may not be predictable at all from a local measure of orthogonal divergence near the streamline. For the purpose of tractography visualization, however, other streamlines that overlap with the "cone of uncertainty" around the target streamline may be taken as possible future deviating trajectories, and the uncertainty measure may be updated accordingly.

Our model describes deviation due only to image noise, which has a uniform effect throughout the brain. It does not yet incorporate the effect of true FA or MD on reconstruction uncertainty. It is thus less specific than the technique of Jones [3], but is easier to implement, far less computationally intensive, and more directly applicable to tractography.

Conclusion — We find that the angular deviation of reconstructed diffusion tensors from the ground truth follows a Rayleigh distribution with scale parameter proportional to the DWI noise level and inversely proportional to the square root of the number of b-vectors. We also find that orthogonal deviations on a tractography streamline are independent on a length scale equal to twice the width of a voxel, when using cubic interpolation in the tractography algorithm. As a result, we find that streamline uncertainty (quantified by the Rayleigh scale parameter σ) accumulates with the square root of arc length away from the seed point.

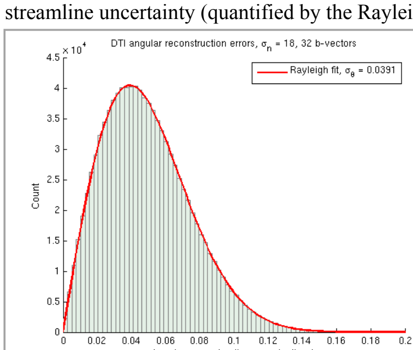

Figure A. Experiment 1 angular differences.

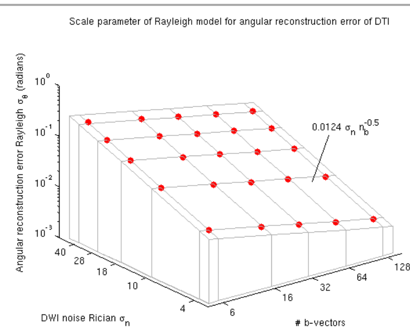

Figure B. Experiment 1 σ_θ regression.

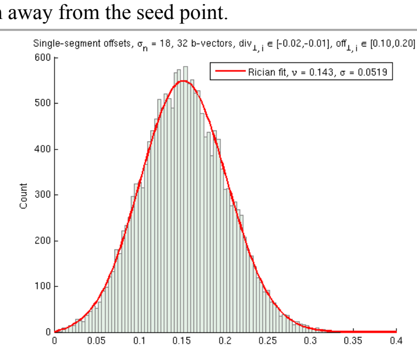

Figure C. Experiment 2 orthogonal offsets.

[1] Press, et al. Numerical Recipes, 3rd ed, 2007. [2] Laun, et al. Magn Reson Mater Phy 22(3), 2009. [3] Jones. MRM 49(1), 2003.